Karadeniz Fen Bilimleri Dergisi, 15(3), 1119-1132, 2025. DOI: 10.31466/kfbd.1617959

KFBD

Karadeniz Fen Bilimleri Dergisi
The Black Sea Journal of Sciences
ISSN (Online): 2564-7377 https://dergipark.org.tr/tr/pub/kfbd

Araştırma Makalesi / Research Article

Photocharacterization and pH Sensing Properties of a Novel Synthesized Fluorescent Schiff Base Derivative

Merve ZURNACI[1*]

Abstract

Design and synthesis of different, highly sensitive and fast response fluorescent materials are very important in the development of pH sensors. In this study, a new pH-sensitive Schiff-base ligand (PHS1) was synthesized by the condensation reaction of newly synthesized 1,3,4-thiadiazole derivative containing phenanthroimidazole (PHT1) with 3,5-ditertbutylsalicylaldehyde (1:1) in ethanol. The molecular structure was confirmed by structural characterization methods. The absorption and fluorescence properties of PHS1 were investigated in DMSO to determine the photocharacterization properties. Then, PHS1 was investigated as a fluorescent pH sensor. UV absorption and emission studies of PHS1 with varying pH (at pH=2.0, 4.0, 6.0, 8.0, 10.0 and 12.0) were determined in Britton-Robinson buffer. The absorption wavelength recorded at 345 nm at pH 2.0 showed bathochromic effect as pH increased (at pH= 4.0; 6.0 and 8.0). At pH 10.0 and 12.0, PHS1 showed two absorption peaks at 357 nm and a new low energy absorption band at 405 nm. The fluorescence spectrum of PHS1 showed a red shift with an increasing wavelength from 439 nm to 473 nm between pH=2.0 and 12.0. These results showed that PHS1 is sensitive to pH change in acidic and basic environments.

Keywords: Schiff Base Derivative, pH Sensor, Photocharacterization, UV-Vis absorption, Fluorescence.

Yeni Sentezlenen Floresan Schiff Bazı Türevinin Fotokarakterizasyonu ve pH Algılama Özellikleri

Öz

pH sensörlerinin geliştirilmesinde, farklı, yüksek hassasiyet ve hızlı tepki floresan malzemelerin tasarımı ve sentezi çok önemlidir. Bu çalışmada, yeni sentezlenen fenantroimidazol içeren 1,3,4-tiyadiazol türevinin (PHT1) etanolde 3,5-ditertbütilsalisilaldehit (1:1) ile kondenzasyon reaksiyonu ile yeni bir pH-duyarlı Schiff bazı ligandı (PHS1) sentezlendi. Moleküler yapı, yapısal karakterizasyon yöntemleri ile doğrulandı. PHS1'in absorpsiyon ve floresan özellikleri, fotokarakterizasyon özelliklerini belirlemek için DMSO'da incelendi. Daha sonra, PHS1 floresan pH sensörü olarak araştırıldı. PHS1'in değişen pH'ta (pH=2,0, 4,0, 6,0, 8,0, 10,0 ve 12,0'da) UV absorpsiyon ve emisyon çalışmaları Britton-Robinson tamponunda belirlendi. pH 2,0'de 345 nm'de kaydedilen emilim dalga boyu, pH arttıkça batokromik etki gösterdi (pH= 4,0'da; 6,0 ve 8,0). pH 10,0 ve 12,0'de, PHS1 357 nm'de iki emilim tepe noktası ve 405 nm'de yeni bir düşük enerjili emilim bandı gösterdi. PHS1'in floresan spektrumu pH=2,0-12,0 arasında 439 nm'den 473 nm'ye artan bir dalga boyu ile kırmızıya kayma gösterdi. Bu sonuçlar PHS1'in asidik ve bazik ortamlardaki pH değişimine duyarlı olduğunu gösterdi.

Anahtar Kelimeler: Schiff Bazı Türevi, pH Sensörü, Fotokarakterizasyon, UV-Vis absorpsiyonu, Floresans.

[1] Kastamonu University, Central Research Laboratory, Kastamonu, TURKEY, mzurnaci@kastamonu.edu.tr

[*] Sorumlu Yazar/Corresponding Author

Geliş/Received: 11.01.2025 **Kabul/Accepted:** 25.08.2025 **Yayın/Published:** 15.09.2025

Zurnacı, M. (2025). Photocharacterization and pH Sensing Properties of a Novel Synthesized Fluorescent Schiff Base Derivative. *Karadeniz Fen Bilimleri Dergisi*, 15(3), 1119-1132.

1. Introduction

pH sensing plays a critical role in many areas such as monitoring biological-chemical processes, industrial control mechanisms and environmental analysis (Baldini, 1999). In this context, the development of new fluorescent sensors offering high sensitivity, selectivity and stability is an important focus of scientific studies (Belko et al., 2023; Li et al., 2024). In recent years, significant progress has been made in fluorescent sensor technology using innovative materials such as nanomaterials, biocompatible polymers and organic dyes (Ma et al., 2017; Mao et al., 2019; Xiao et al., 2021). Among fluorescent sensors, Schiff bases stand out as versatile receptors that differ in terms of fluorescence properties, binding abilities and selective recognition depending on the structure of the amine and aldehyde (Musikavanhu, Liang, Xue, Feng, & Zhao, 2023; Yıldırım & Yıldız, 2018). Additionally, Schiff base derivatives are considered as potential candidates for the design of fluorescent sensors that can operate effectively over a wide pH range (Halder, Hazra, & Roy, 2018; Kaya, Aydın, & Yıldırım, 2012).

Schiff bases (known as imines or azomethines) have an important place in a wide range of applications as organic molecules formed by the condensation of primary amines with compounds containing carbonyl groups (**Fig 1**) (Berhanu et al., 2019; Pervaiz et al., 2024). Thanks to their structural diversity and fastly synthesizability, these compounds have attracted attention especially in the development of chemical sensors and materials with photophysical properties (Kumar et al., 2022). The fluorescent properties of Schiff bases offer a special advantage for pH sensing applications due to their high sensitivity to environmental factors (Halder et al., 2018).

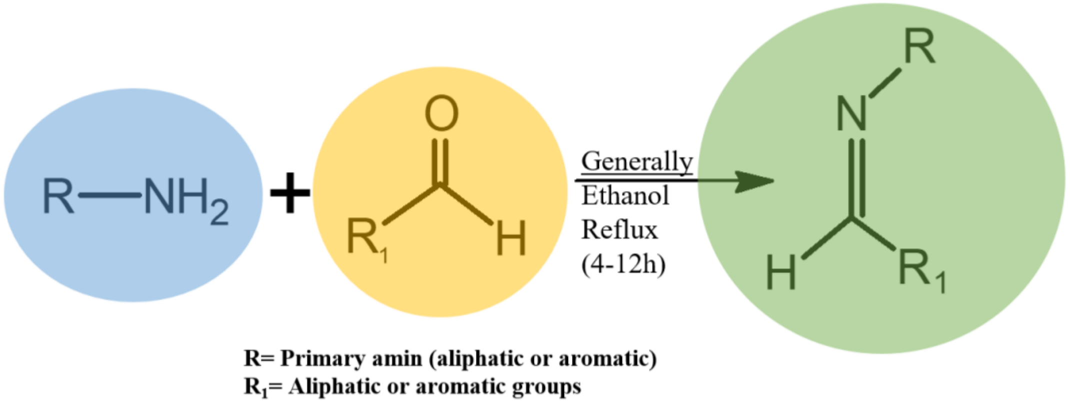

Figure 1. General synthesis reaction of Schiff bases

The presence of an -OH group in the structure of Schiff bases significantly affects the behaviour of the molecule as a fluorescence pH sensor (Maity, Halder, & Roy, 2018). The imine group (-C=N-) and the phenolic -OH group of the Schiff base usually form delocalized π-electron systems. Energy absorption occurs as a result of π-π* or n-π* transitions and this energy is dissipated through fluorescence (Huang, Ding, Bi, Yu, & Zeng, 2021). The presence of the -OH group triggers the excited-state intramolecular proton transfer (ESIPT) mechanism in the Schiff base molecule (Shu et al., 2021). In the excited state, the proton (H^+) is transferred from the phenolic group to the imine. Thanks to ESIPT, Schiff bases take part in the detection of solvent environment, pH changes or metal ions (Silva, Canisares, Mutti, Pires, & Lima, 2023). The -OH group affects the electron density by supporting the proton transfer mechanisms. All these processes cause changes in the fluorescence properties of the molecule and create differences in the characteristic emission wavelengths (Maity et al., 2018).

There are numerous articles in the literature about the pH sensing activities of Schiff bases (Halder et al., 2018; Kaya et al., 2012; Maity et al., 2018; Silva et al., 2023). Especially Schiff bases with aromatic structures containing π-conjugated systems are frequently encountered as pH sensors (Bhardwaj, Ashok Kumar, & Sahoo, 2022). Dinesh Maity et al. (2018) synthesized a new Schiff base molecule as a pH chemosensor. They emphasized that it showed an emission at 571 nm up to pH 10.5 and a new peak appeared at 504 nm with changing pH. They found that the color of the Schiff base changed significantly when the pH of the aqueous medium changed from 10.5 to 11 when observed under both visible and UV light (Maity et al., 2018). Shibashis Halder et al. (2017) studied the colorimetric and fluorescence sensing of pH by a Schiff-base molecule. They carried out absorption and emission measurements of the synthesized Schiff base in the pH range of 2.0–11.0. In the UV-Vis spectrum, it showed high absorption at 358 nm at pH 2.0. They reported that the intensity of this band decreased with the increase in pH. They also found that a new absorption band appeared at 430 nm. They stated that the high emission intensity and fluorescence peak were at 464 nm at low pH. They found that the intensity decreased with the increase in pH and a new peak appeared at 529 nm (Halder et al., 2018).

In this study, the photocharacterization properties of a newly synthesized fluorescent Schiff base derivative were investigated in detail and its pH sensing capacity was investigated. The findings regarding the photocharacterization, fluorescence determination and pH sensitivity of the compound are thought to shed light on both theoretical and practical applications. The obtained results reveal the potential of this new derivative to be used as a pH sensor.

2. Materials and Methods

2.1. Chemicals and Instrumentations

9,10-phenanthreneqinone, 4-formylbenzoic acid, thiosemicarbazide and 3,5-ditertbutylsalicilaldehyde used in the synthesis. This chemicals and solvents were used spectroscopic grade (>%99). **Structural characterization**: ^{1}H-NMR measurements were carried out by Agilent

Premium Compact 600 MHz (14.1 Tesla) NMR spectrometer. FT-IR analyses were performed using Bruker Alpha. Mass and product ion scanning studies were recorded using the Shimadzu brand LCMS-MS/8030 Plus model (LCMS-MS). **Photocharacterization**: UV-Vis (Shimadzu UV Pharmaspec) and Fluorescence (Horiba Fluoromax-4) Spectrophotometers investigated the absorption and emission properties. **Quantum yield measurements:** Perylene ($C_{20}H_{12}$, Sigma-Aldrich, >%99). **pH sensing studies**: Britton-Robinson buffer (glacial acetic acid (%99-CH_3COOH), phosphoric acid (%85- H_3PO_4), boric acid (H_3BO_3), sodium hydroxide (NaOH) and deionized water).

2.2. Synthesis and Structural Characterization Fluorescent pH Sensor (PHS1)

Stage 1: 4-(1*H*-phenanthro[9,10-d]imidazole-2-yl)benzoic acid was obtained by the condensation reaction between aldehyde and phenanthrenequinone (Hwang, Chae, & Kim, 2018). The reaction was carried out using ammonium acetate and glacial acetic acid (%99.9). As a result, 4-(1H-phenanthro[9,10-d]imidazole-2-yl)benzoic acid was obtained, with yields of 91%. By this method, phenanthro[9,10-d]imidazole compound was synthesized in high yield without using any catalyst (Hwang et al., 2018).

Stage 2: In the last part of the synthesis steps, the reaction of 4-(*1H*-Phenanthro[9,10-d]imidazole-2-yl)benzoic acid compound and thiosemicarbazide was carried out (Zurnacı, Şener, Gür, & Şener, 2022). Thus, the synthesis of a 1,3,4-thiadiazole derivative containing phenanthroimidazole structure was carried out. 4-(*1H*-phenanthro[9,10-d]imidazole-2-yl)benzoic acid (0.5 g, 1.5 mmol), thiosemicarbazide (0.137 g, 1.5 mmol) and $POCl_3$ (0.42 mL, 4.5 mmol) were added into 50 mL round-bottomed flask. Reaction conditions: 4-5 hours and 90 °C. The resulting mixture was precipitated with ice water. The mixture was adjusted with ammonia (%20) to pH=7-8 the next day. This compound was obtained as a light brown solid and dried.

Stage 3: In the final stage, 0.24 gr of PHT1 (0.6 mmol) and 0.14 gr of 3,5-ditertbutylsalicylaldehyde (0.6 mmol) were dissolved in 30 mL of ethanol. The mixture was refluxed for 5-6 hours. Glacial acetic acid was then added dropwise to the mixture to bring the pH to 4-5 (Silva et al., 2023). The precipitate formed at the end of the reaction was washed with plenty of water and filtered, and passed through diethyl ether to dry easily and to prevent contamination. The route of synthesis is given in **Fig 2**.

Afterwards, preliminary analysis procedures such as melting point determination and thin layer chromatography were performed. Experimental data are given in **Table 1**. The progress was made in the light of the spectroscopic methods determined for structural characterization. All structural characterization data are given in detail in the **Supplementary File**. In the FT-IR spectrum, the peak that is one of the characteristic peaks of Schiff bases and is generally observed in the range of 1640-

1690 cm^{-1} is clearly seen (Namli & Turhan, 2006). The peak seen at 1644.04 corresponds to the C=N (imine group) stretching vibrations (**Sup. Fig S1**). Yield: (87%), melting point (mp): 310 °C; **FT-IR (cm^{-1}) ν**: 3051.50 cm^{-1} (aromatic, C-H) stretching, –NH), 2955.54; 2865.83 cm^{-1} (aliphatic, C-H), 1644.04 cm^{-1} (-C=N-, imine); 1611.71 cm^{-1} (-C=C-), 751.10 cm^{-1} (-C-S-C-). **^{1}H-NMR (600 MHz, DMSO-d6, δ/ppm):** 10.98 (1H, ─NH), 8.80-6.90 (4H, aromatic protons), 2.90-1.70 (20H, aliphatic protons) detailed in **Sup. Fig S2. ^{13}C-NMR ppm (600 MHz, DMSO-d6, δ/ppm)**: 200.0 (1C, ─OH), 170.0-112.0 (28H, aromatic protons), 68.0 (1C, -C=N-, imine);), 38.0-25.2 (8H, aliphatic protons) detailed in **Sup. Fig S3. LCMS-MS (ESI-m/z) (M+H)$^{+}$**: Calculated/found: 609.79/609.10 detailed in **Sup. Fig S4**.

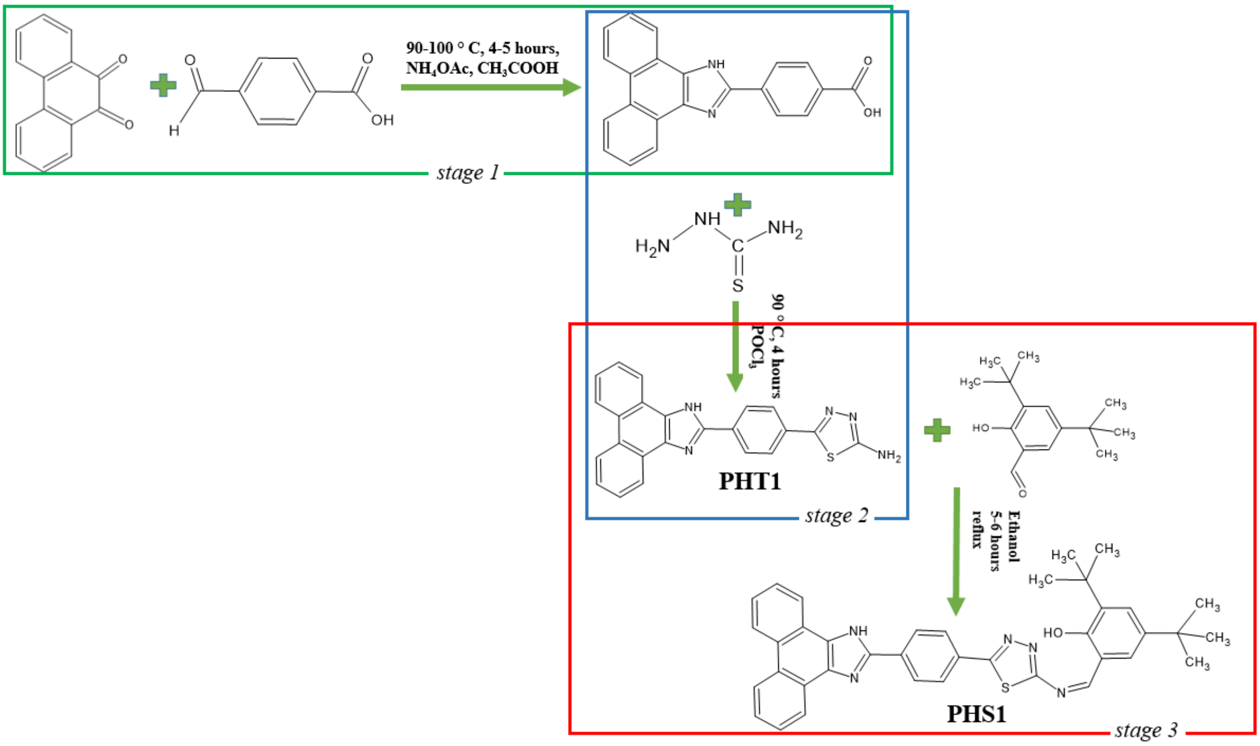

Figure 2. Synthesis route of PHS1

Table 1. Experimental data of PHS1

Molecular structure	Molecular formula	Molecular weight (g/mol)	Yield (%)	Melting point (^{0}C)
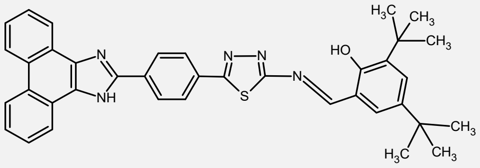	$C_{38}H_{35}N_5OS$	609.78	%87	310 ^{0}C

3. Findings and Discussion

3.1. Photocharacterization Studies

UV-Vis absorption measurements were performed on a Shimadzu model UV-1700 spectrometer in a 1 cm quartz cuvette with an overall spectral range of 700-200 nm and 1 nm intervals. Emission spectra of PHS1 were obtained on a Horiba Fluoremax-4 model steady-state fluorescence spectrophotometer. The emission slit interval was 1 nm, and the integration (measurement) time was 0.1 s. UV-vis and photoluminescence measurements of PHS1 were carried out at room temperature (298 K) in the DMSO.

The absorption and emission spectra of PHS1 in DMSO at 4x10^{-5} molL^{-1} under steady state conditions are given in Fig. 3. The absorption wavelengths of PHS1 were determined as 291, 310, 349 and 365 nm, respectively. The fluorescence emission wavelength was 447 nm and the Stokes shift value was 82 **(Fig 3)**. Since Schiff bases generally have π-π* and n-π* transitions, their absorption spectra depend on the energies of these transitions (Payal, Saroj, Sharma, & Rastogi, 2018). The imine (-C=N-) group of the Schiff base exhibits n-π* transitions due to the non-bonding (n) electron pairs on nitrogen. These transitions usually occur in the UV region because they have lower energy (Shatir, Aly, Ebrahium, Saddeek, & Ranjith Kumar, 2024). In addition, the bond structure of the imine group affects the electron density of the Schiff base. This can change the shape and position of the absorption spectrum. Side groups attached to the imine group can also change the characteristics of the spectrum (Raczuk, Dmochowska, Samaszko-Fiertek, & Madaj, 2022).

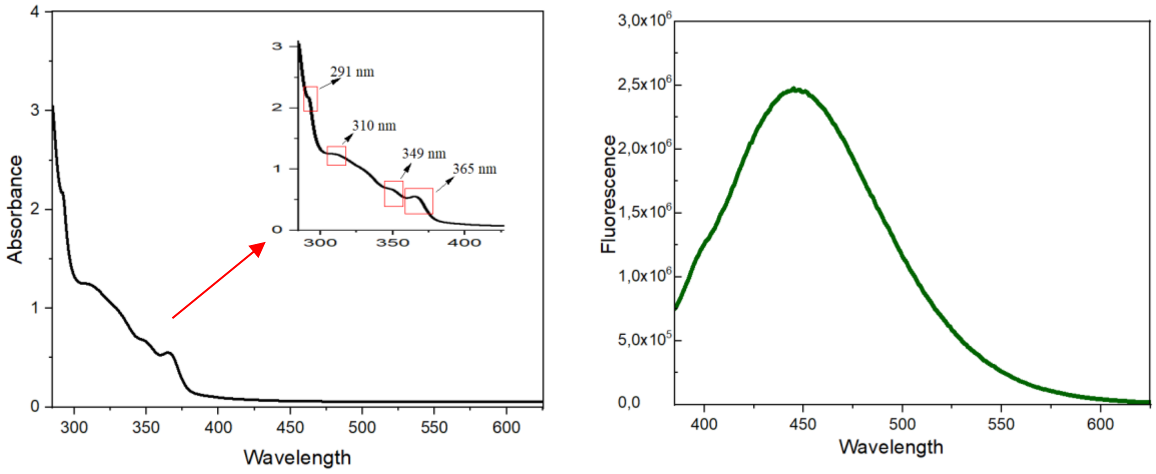

(a) (b)

Figure 3. Absorption (a) and emission (b) spectra of PHS1 in DMSO (4x10^{-5} molL^{-1}, steady-state measurements, λ_{exc}=365 nm)

The quantum yield was calculated by comparing with a known reference. For this, the same concentration and the same conditions were studied. The quantum yields of Schiff base derivative

(PHS1) were measured in the same equipment using Perylene as a reference (Φ = 0.94 – in cyclohexane) (Brouwer, 2011). While determining the quantum yield of PHS1, the slit interval was set as ex.: 1 nm; em.: 1 nm, integration time: 0.1 s. The reference and PHS1 integration area was calculated in Origin 2018. The refractive indices of the solvents used in the quantum yield measurements were 1.479 and 1.426 for DMSO and cyclohexane, respectively. The quantum yield of PHS1 was calculated using the above data and the quantum yield equation (Equation 1). **Fig 4** shows the integration graph of the emission spectrum of PHS1 in DMSO (I_s=1.30083 E7). As shown in **Table 2**, the quantum yield of *PHS1* was 0.25 (%25) in the DMSO. The color change of PHS1 in DMSO under daylight and UV light (365nm) is seen in **Fig 5.** PHS1, which is transparent in daylight, was observed to be blue under UV light in the dark.

$$\mathrm{Q}_S = \frac{A_R\, I_S\, (n_S)^2}{A_S\, \mathrm{R}\, (n_R)^2} \mathrm{Q}_R \qquad (1)$$

Q: Quantum yield
S: Sample (*PHS1*)
R: Reference
A: Absorbance measured at excitation wavelength
I: Emission area
n: Refractive index

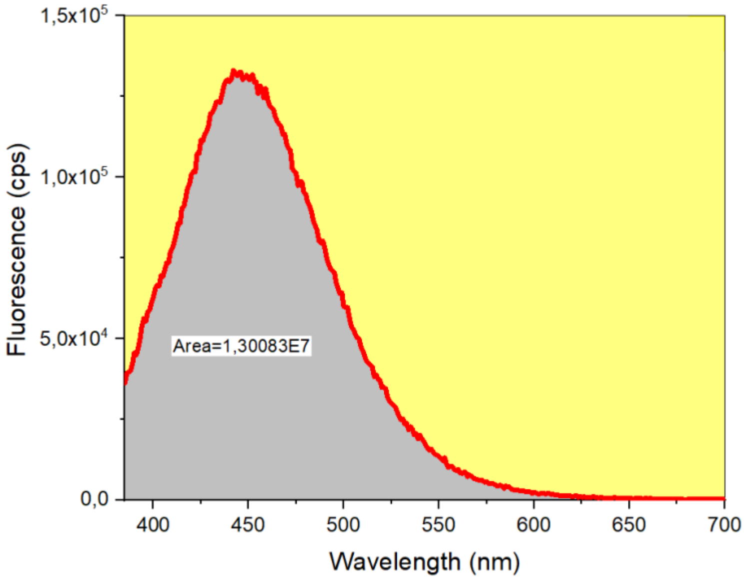

Figure 4. Integration of emission spectrum of PHS1 in DMSO (1x10^{-5} molL^{-1} and slit=1 nm)

Figure 5. Color changes (day light-365 nm UV light) of the PHS1 in DMSO

Table 2. Photocharacterization properties for PHS1 in DMSO (1x10^{-5} M)

	Absorption (λ)	Absorbance (A)	Excitation (λ)	Emission (λ_{max})	Intensity (cps)	Stokes' Shift (λ)	Quantum Yield (Q_f)
PHS1	365	0.148	365	447	130180	82	0.253

3.2. pH Sensing Studies

There are two situations during pH change: protonation and deprotonation. Protonation generally shifts the absorption peaks to shorter wavelengths (blue shift, hypsochromic shift) (Alata, Broquier, Dedonder, Jouvet, & Marceca, 2012; Grante, Actins, & Orola, 2014). During protonation, the effect of non-bonding electrons on nitrogen decreases, which can weaken the n-π* transition or cause peaks to disappear in the spectrum. Deprotonation generally increases the absorption intensity because the -O⁻ form exhibits electron donor properties and provides a stronger interaction with the π-system (Halder, Bhattacharjee, Roy, Chatterjee, & Roy, 2016; Halder et al., 2018). The non-bonding electron pairs (n orbital) on the imine group (-C=N-) in the structure of Schiff bases may show different interactions depending on the pH change (Halder, Dey, & Roy, 2015). In the case of deprotonation, the energy levels of the n-π* transitions may change and the absorption wavelengths may shift. The "Receptor-Spacer-Fluorophore" scheme for PHS1 is shown in **Scheme 1**.

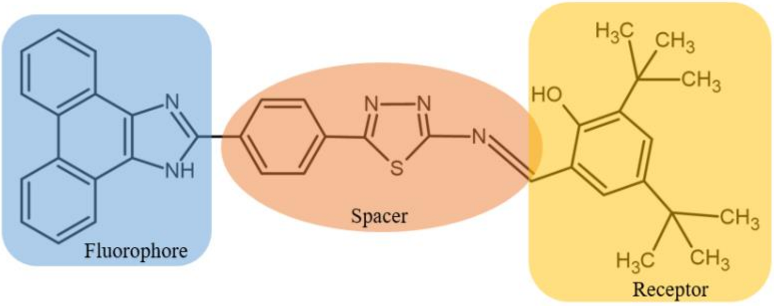

Scheme 1. The "Receptor-Spacer-Fluorophore" design for PHS1

In this study, Britton-Robinson buffer solution was used for UV absorption and emission studies of PHS1 with pH change. B-R buffer was prepared as 1 L stock solution by calculating 0.04 molL-1 each of phosphoric acid, boric acid and acetic acid. 0.2 molL^{-1} NaOH was slowly added to adjust the pH of the buffer to the desired value (Nantaphol, Chailapakul, & Siangproh, 2015). Afterwards, the pH of B-R buffer solutions was prepared as 2.0, 4.0, 6.0, 8.0, 10.0, 12.0 with the help of a pH meter. 3 mL of buffer solutions with different pHs were taken. 1 mL of PHS1 was added to these buffer solutions (PHS1 was prepared as 4×10^{-5} mol L^{-1} in DMSO). 6 series of samples with a molarity of

1×10^{-5} mol L^{-1} were obtained. The mixture was well dissolved with the help of vortex and immediately transferred to quartz cuvette. UV-vis and fluorescence measurements were performed.

UV–Vis absorption spectra of PHS1 in 1×10^{-5} mol L^{-1} were obtained in B–R buffer at room temperature, from pH 2.0 to 12.0 (**Fig 6**). Although the absorption spectra at different pHs show similar behaviour, there are a few points that are noteworthy. The absorption wavelength recorded at 345 nm at pH 2.0. As the pH increases (at pH= 4.0; 6.0 and 8.0), the wavelength showed at 345 nm occurs bathochromic effect. The absorption spectra measured at pH=4.0; 6.0 and 8.0 is very similar (λ_{max}=358 nm).

At pH 10.0 and 12.0, PHS1 presented two absorption peaks. The first one is centered at approximately 357 nm. Simultaneously, a new lower-energy absorption band is observed at 405 nm. The absorption spectra recorded between pH 10.0 and 12.0 evidence a new band at 405 nm, caused by the intramolecular charge transfer since the ionized species has its concentration increased in this interval. It was previously emphasized that as the pH increases, the -OH group in the structure of the Schiff base is deprotonated and converted to the $-O^{-}$ form, which expands the conjugation of the molecule. This result has proven its accuracy. It is seen in Fig. 6 that the π-π* transitions shift to longer wavelengths. It is also clearly seen that deprotonation generally increases the absorption intensity. While the absorbance is 0.140 (purple curve in **Fig 6**) at pH=10, it is 0.25 (yellow curve in **Fig 6**) at pH=12.

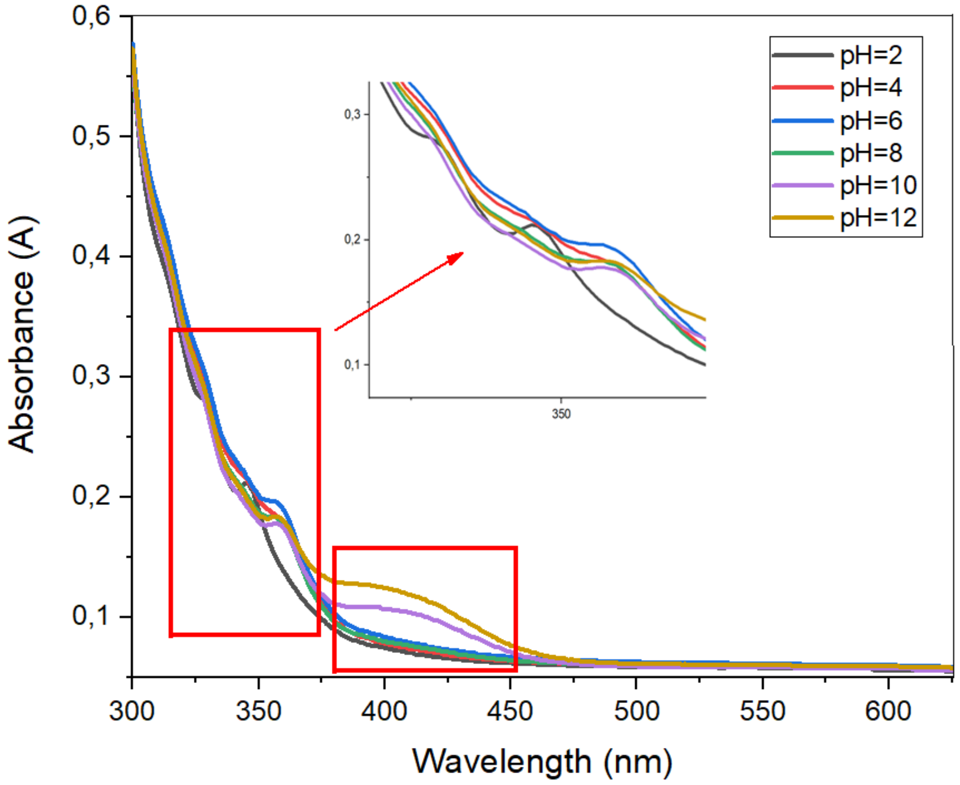

Figure 6. Absorption spectra of PHS1 at pH=2.0-12.0 in B-R buffer ($1x10^{-5}$ $molL^{-1}$)

Fluorescence properties generally vary depending on the chemical structure of the Schiff base, the location of the -OH group, and the general electronic properties of the molecule (Musikavanhu et al., 2023). pH changes can cause the molecule to transition between different tautomeric forms (e.g. keto-enol transition) (Khandogin & Brooks, 2005). This leads to changes in the fluorescence properties of the molecule and the bands in the emission spectrum. When examining the fluorescence properties, protonation generally causes the emission wavelength to shift to blue; deprotonation generally causes the emission wavelength to shift to red (Ryazanova, Voloshin, Makitruk, Zozulya, & Karachevtsev, 2007). In this study, red-shifted emissions are observed at high pH. The emission spectrum and pH-dependent emission intensities of PHS1 are given in **Fig 7**. The maximum fluorescence wavelength is observed at approximately 439-473 nm. When the emission wavelengths of PHS1 were examined, it was seen that it was the highest at pH = 12 and the lowest at pH = 2. The emission wavelengths measured at pH = 4.0, 6.0 and 8.0 are very close to each other. The emission wavelengths of the compounds were pH = 12 (473) > pH = 10.0 (469) > pH = 8.0 (469) > pH = 6.0 (468) > pH = 4.0 (465) > pH = 2.0 (439), respectively **(Table 3)**.

The highest fluorescence intensity was observed at pH=2.0 (black curve). As pH increases, there is a significant decrease in fluorescence intensity towards pH=12.0 (yellow curve). While the emission intensity is 46990 cps at pH=2.0, the lowest value is 22280 cps at pH=12.0. This shows that the fluorescence properties of the molecule are clearly affected by the pH change. Color changes of PHS1 in B-R buffer solution at pH = 2.0-12.0 (daylight-365 nm UV light) are seen in **Fig 8**.

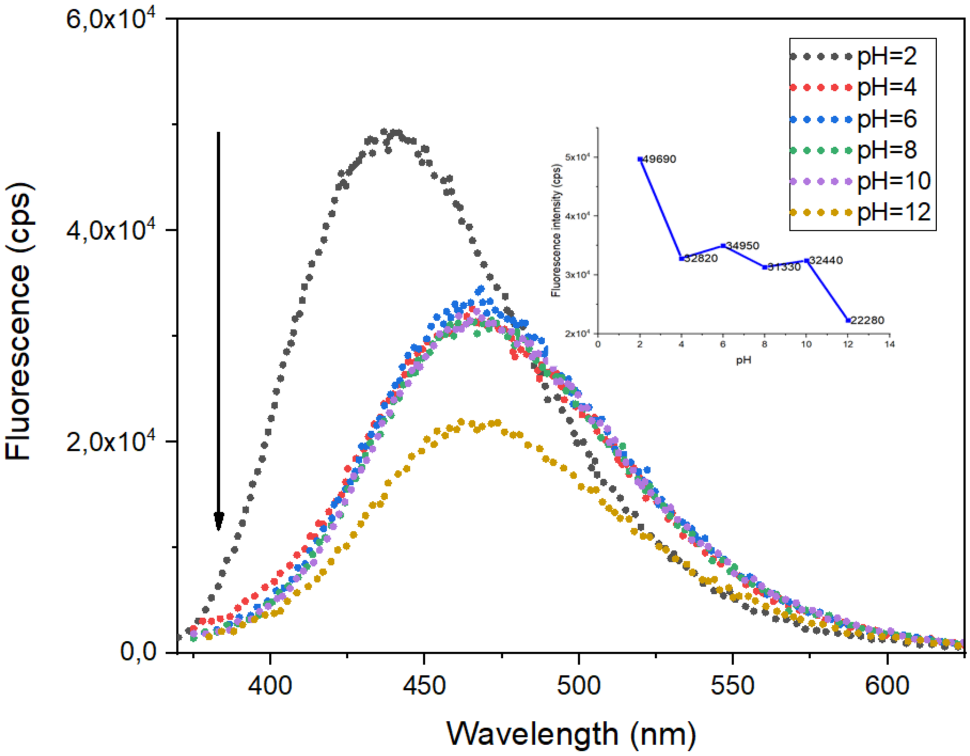

Figure 7. Fluorescence spectra and emission intensity-pH of PHS1 at pH=2.0-12.0 in B-R buffer ($1x10^{-5}$ $molL^{-1}$)

Table 3. Photocharacterization properties for PHS1 in different pH ($1x10^{-5}$ M)

	Absorption (λ)	Absorbance (A)	Excitation (λ)	Emission (λ_{max})	Intensity (cps)	Stokes' Shift (λ)
pH=2	345	0.212	345	439	49690	94
pH=4	358	0.180	359	465	32820	106
pH=6	358	0.194	358	468	34950	110
pH=8	358	0.191	358	469	31330	111
pH=10	357;405	0.178	357	469	32440	112
pH=12	357;405	0.183	357	473	22280	116

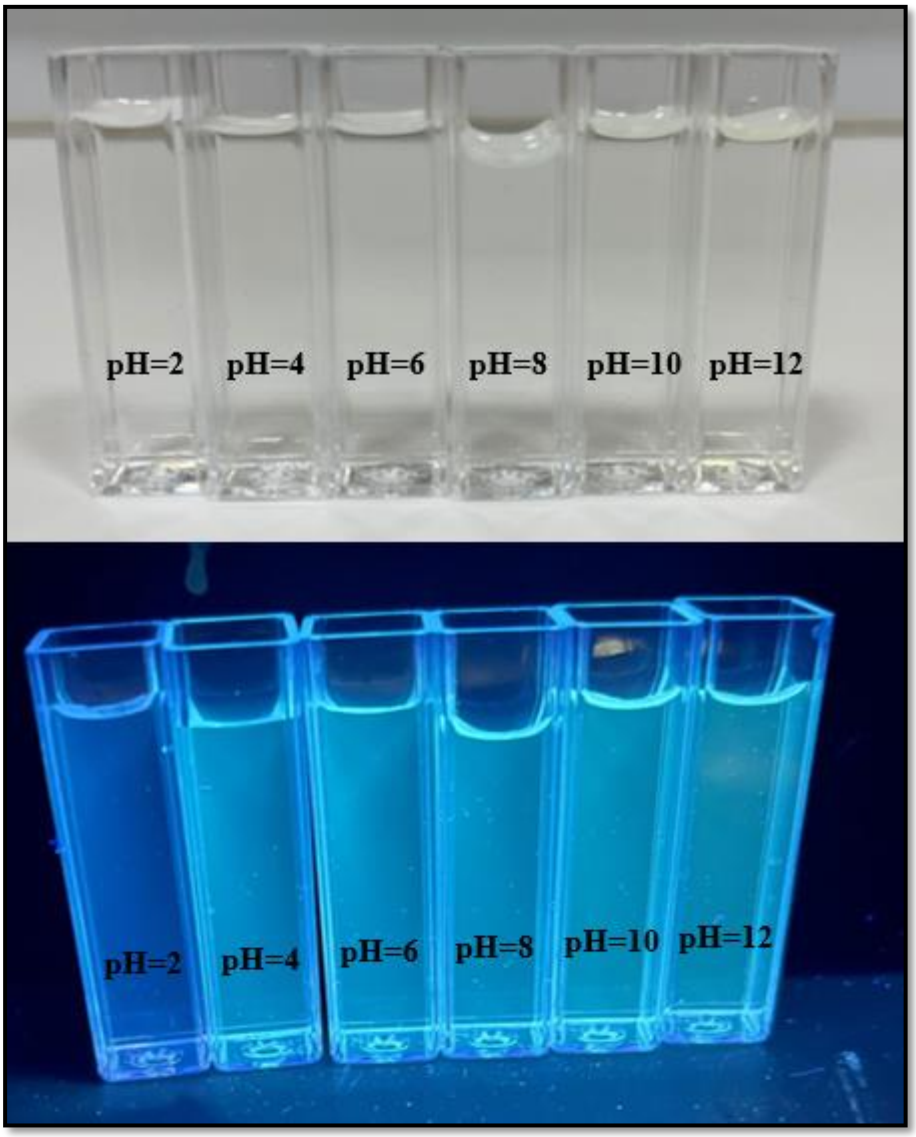

Figure 8. Color changes (day light-365 nm UV light) of the PHS1 at pH=2.0-12.0 in B-R buffer solution

4. Conclusions and Recommendations

In this study, the photocharacterization and pH sensing properties of the newly synthesized fluorescent Schiff base derivative PHS1 were investigated comprehensively. The absorption and emission spectra of the compound exhibited significant differences depending on pH changes. The obtained results support the usability of this molecule as a potential pH sensor. In the UV-Vis absorption spectra, the protonation/deprotonation balance of the molecule and the related intramolecular charge transfer were effective with the increase in pH. In particular, the emergence of a new low-energy absorption band at 405 nm at pH ≥ 10.0 levels indicates this situation. In addition, the increase in absorption intensity observed between pH 10.0 and 12.0 is compatible with the deprotonation processes of the Schiff base. When the fluorescence properties were examined, it was observed that at low pH levels caused a blue shift in the emission wavelength, while at high pH levels shifted the emission to red. These results show that the fluorescence properties of the molecule are strongly affected by pH changes, both in terms of emission wavelength and intensity.

Overall, this study reveals the relationship between the chemical structure and photophysical behaviour of the PHS1, while also highlighting the potential of this compound to be used as an effective pH sensor in a wide pH range. The findings show that the molecule can contribute to the development of new generation pH sensors in applied fields. Future studies envisage the investigation of the behaviour of such Schiff base derivatives in different solvents, as well as their performance in biological and environmental applications.

Authors' Contributions

All processes of the study were carried out by the author, Merve ZURNACI.

Statement of Conflicts of Interest

There is no conflict of interest.

Statement of Research and Publication Ethics

The author declares that this study complies with Research and Publication Ethics.

References

Alata, I., Broquier, M., Dedonder, C., Jouvet, C., & Marceca, E. (2012). Electronic excited states of protonated aromatic molecules: Protonated Fluorene. *Chemical Physics*, *393*(1), 25–31. https://doi.org/10.1016/j.chemphys.2011.11.013

Baldini, F. (1999, February 23). *Critical review of pH sensing with optical fibres* (R. A. Lieberman, ed.). https://doi.org/10.1117/12.339779

Belko, N., Maltanava, H., Lugovski, A., Ferreira, R. A. S., Correia, S. F. H., Shabunya, P., … Samtsov, M. (2023). pH-Sensitive fluorescent sensor for Fe(III) and Cu(II) ions based on rhodamine B acylhydrazone: Sensing mechanism and bioimaging in living cells. *Microchemical Journal*, *191*, 108744. https://doi.org/10.1016/j.microc.2023.108744

Berhanu, A. L., Gaurav, Mohiuddin, I., Malik, A. K., Aulakh, J. S., Kumar, V., & Kim, K.-H. (2019). A review of the applications of Schiff bases as optical chemical sensors. *TrAC Trends in Analytical Chemistry*, *116*, 74–91. https://doi.org/10.1016/j.trac.2019.04.025

Bhardwaj, V., Ashok Kumar, S. K., & Sahoo, S. K. (2022). Fluorescent sensing (Cu2+ and pH) and visualization of latent fingerprints using an AIE-active naphthaldehyde-pyridoxal conjugated Schiff base. *Microchemical Journal*, *178*, 107404. https://doi.org/10.1016/j.microc.2022.107404

Brouwer, A. M. (2011). Standards for photoluminescence quantum yield measurements in solution (IUPAC technical report). *Pure and Applied Chemistry*, *83*(12), 2213–2228. https://doi.org/10.1351/PAC-REP-10-09-31

Grante, I., Actins, A., & Orola, L. (2014). Protonation effects on the UV/Vis absorption spectra of imatinib: A theoretical and experimental study. *Spectrochimica Acta Part A: Molecular and Biomolecular Spectroscopy*, *129*, 326–332. https://doi.org/10.1016/j.saa.2014.03.059

Halder, S., Bhattacharjee, A., Roy, A., Chatterjee, S., & Roy, P. (2016). Chromogenic and fluorescence sensing of pH with a Schiff-base molecule. *RSC Adv.*, *6*(45), 39118–39124. https://doi.org/10.1039/C6RA06284A

Halder, S., Dey, S., & Roy, P. (2015). A quinoline based Schiff-base compound as pH sensor. *RSC Advances*, *5*(68), 54873–54881. https://doi.org/10.1039/C5RA07538F

Halder, S., Hazra, A., & Roy, P. (2018). Colorimetric and fluorescence sensing of pH with a Schiff-base molecule. *Journal of Luminescence*, *195*, 326–333. https://doi.org/10.1016/j.jlumin.2017.11.055

Huang, S., Ding, J., Bi, A., Yu, K., & Zeng, W. (2021). Insights into Optical Probes Based on Aggregation-Induced Emission: from Restriction of Intramolecular Motions to Dark State. *Advanced Optical Materials*, *9*(21). https://doi.org/10.1002/adom.202100832

Hwang, S. M., Chae, J. B., & Kim, C. (2018). A Phenanthroimidazole-based Fluorescent Turn-Off Chemosensor for the Selective Detection of Cu2+ in Aqueous Media. *Bulletin of the Korean Chemical Society*, *39*(8), 925–930. https://doi.org/10.1002/bkcs.11526

Kaya, İ., Aydın, A., & Yıldırım, M. (2012). Synthesis and Spectrophotometric PH Sensing Applications of Poly-2-[4-(diethylaminophenyl)imino]-5-nitro-phenol and its Schiff Base Monomer for Two Different PH Ranges. *Journal of Fluorescence*, *22*(1), 495–504. https://doi.org/10.1007/s10895-011-0983-3

Khandogin, J., & Brooks, C. L. (2005). Constant pH Molecular Dynamics with Proton Tautomerism. *Biophysical Journal*, *89*(1), 141–157. https://doi.org/10.1529/biophysj.105.061341

Kumar, A., Virender, Saini, M., Mohan, B., Shayoraj, & Kamboj, M. (2022). Colorimetric and fluorescent Schiff base sensors for trace detection of pollutants and biologically significant cations: A review (2010–2021). *Microchemical Journal*, *181*, 107798. https://doi.org/10.1016/j.microc.2022.107798

Li, S.-S., Zhou, H.-T., Li, H.-Z., Zhong, L.-C., Zhang, F.-H., Sun, F.-B., … Zheng, Y.-C. (2024). Recent advances in the development of fluorescent sensors for sulfur mustard detection. *Journal of Materials Chemistry C*, *12*(27), 9914–9928. https://doi.org/10.1039/D4TC01159G

Ma, C., Xie, G., Zhang, X., Yang, L., Li, Y., Liu, H., … Wei, Y. (2017). Biocompatible fluorescent polymers from PEGylation of an aggregation-induced emission dye. *Dyes and Pigments*, *139*, 672–680. https://doi.org/10.1016/j.dyepig.2016.12.070

Maity, D., Halder, S., & Roy, P. (2018). High pH Sensing Properties of a New Schiff-base Compound. *ChemistrySelect*, *3*(2), 440–445. https://doi.org/10.1002/slct.201702307

Mao, L., Liu, Y., Yang, S., Li, Y., Zhang, X., & Wei, Y. (2019). Recent advances and progress of fluorescent bio-/chemosensors based on aggregation-induced emission molecules. *Dyes and Pigments*, *162*, 611–623. https://doi.org/10.1016/j.dyepig.2018.10.045

Musikavanhu, B., Liang, Y., Xue, Z., Feng, L., & Zhao, L. (2023). Strategies for Improving Selectivity and

Sensitivity of Schiff Base Fluorescent Chemosensors for Toxic and Heavy Metals. *Molecules*, *28*(19), 6960. https://doi.org/10.3390/molecules28196960

Namli, H., & Turhan, O. (2006). Background defining during the imine formation reaction in FT-IR liquid cell. *Spectrochimica Acta Part A: Molecular and Biomolecular Spectroscopy*, *64*(1), 93–100. https://doi.org/10.1016/j.saa.2005.07.020

Nantaphol, S., Chailapakul, O., & Siangproh, W. (2015). Sensitive and selective electrochemical sensor using silver nanoparticles modified glassy carbon electrode for determination of cholesterol in bovine serum. *Sensors and Actuators B: Chemical*, *207*, 193–198. https://doi.org/10.1016/j.snb.2014.10.041

Payal, R., Saroj, M. K., Sharma, N., & Rastogi, R. C. (2018). Photophysical behavior of some thymol based schiff bases using absorption and fluorescence spectroscopy. *Journal of Luminescence*, *198*, 92–102. https://doi.org/10.1016/j.jlumin.2018.02.007

Pervaiz, M., Shahin, M., Ejaz, A., Quratulain, R., Saeed, Z., Ashraf, A., … Younas, U. (2024). An overview of Aniline-Based Schiff base metal Complexes: Synthesis, characterization and biological activities - a review. *Inorganic Chemistry Communications*, *159*, 111851. https://doi.org/10.1016/j.inoche.2023.111851

Raczuk, E., Dmochowska, B., Samaszko-Fiertek, J., & Madaj, J. (2022). Different Schiff Bases—Structure, Importance and Classification. *Molecules*, *27*(3), 787. https://doi.org/10.3390/molecules27030787

Ryazanova, O. A., Voloshin, I. M., Makitruk, V. L., Zozulya, V. N., & Karachevtsev, V. A. (2007). pH-Induced changes in electronic absorption and fluorescence spectra of phenazine derivatives. *Spectrochimica Acta Part A: Molecular and Biomolecular Spectroscopy*, *66*(4–5), 849–859. https://doi.org/10.1016/j.saa.2006.04.027

Shatir, T. M., Aly, K. A., Ebrahium, M. M., Saddeek, Y. B., & Ranjith Kumar, E. (2024). Linear and non-linear optical and dielectric properties of transition metals complexes films derived from Azo-Schiff base for photovoltaic applications. *Journal of Molecular Liquids*, *401*, 124636. https://doi.org/10.1016/j.molliq.2024.124636

Shu, J., Ni, T., Liu, X., Xu, B., Liu, L., Chu, W., … Jiang, W. (2021). Mechanochromism, thermochromism, protonation effect and discrimination of CHCl3 from organic solvents in a Et2N-substituted Salicylaldehyde Schiff base. *Dyes and Pigments*, *195*, 109708. https://doi.org/10.1016/j.dyepig.2021.109708

Silva, R. C., Canisares, F. S. M., Mutti, A. M. G., Pires, A. M., & Lima, S. A. M. (2023). Small Schiff base molecules derived from salicylaldehyde as colorimetric and fluorescent neutral-to-basic pH sensors. *Dyes and Pigments*, *213*, 111191. https://doi.org/10.1016/j.dyepig.2023.111191

Xiao, D., Qi, H., Teng, Y., Pierre, D., Kutoka, P. T., & Liu, D. (2021). Advances and Challenges of Fluorescent Nanomaterials for Synthesis and Biomedical Applications. *Nanoscale Research Letters*, *16*(1), 167. https://doi.org/10.1186/s11671-021-03613-z

Yıldırım, N., & Yıldız, M. (2018). A Schiff Base Sensor Selective to Anions, Biological Activity and Spectral Studies. *Journal of the Turkish Chemical Society Section A: Chemistry*, *5*(3), 1271–1278. https://doi.org/10.18596/jotcsa.431554

Zurnacı, M., Şener, İ., Gür, M., & Şener, N. (2022). Study on Photophysical Properties of Novel Fluorescent Phenanthroimidazole-Thiadiazole Hybrid Derivatives. *Journal of Fluorescence*, *32*(3), 1155–1169. https://doi.org/10.1007/s10895-022-02916-3